ORIGINAL ARTICLE

Within-tree variability and sample storage effects of bordered pit membranes in xylem of *Acer pseudoplatanus*

Martyna M. Kotowska[1,2] · Rebecca Thom[1] · Ya Zhang[1] · H. Jochen Schenk[3] · Steven Jansen[1]

Abstract

Key message Intervessel pit membranes in xylem tissue of *Acer pseudoplatanus* differ in their thickness both within and across plant organs and may undergo considerable shrinkage during dehydration and sample preparation.

Abstract Intervessel pit membranes have been suggested to account for more than half of the total xylem hydraulic resistance in plants and play a major role in vulnerability to drought-induced hydraulic failure. While the thickness of intervessel pit membranes was found to be associated with xylem embolism resistance at an interspecific level, variation in pit membrane structure across different organs along the flow path within a single tree remains largely unknown. Based on transmission electron microscopy, we examined intra-tree variation of bordered pit and pit membrane characteristics in xylem of roots, stems, branches, petioles, and leaf veins of *Acer pseudoplatanus*. Moreover, potential preparation artefacts on pit membrane structure such as alcohol treatment and dehydration were tested. Our observations showed quantitative differences in bordered pits across organs, including variation in pit membrane thickness within and across organs. Vessel size was weakly related to intervessel wall thickness, but not significantly linked to pit membrane thickness. Gradual dehydration of wood samples resulted in irreversible shrinkage of pit membranes, together with increased levels of aspiration. These findings are relevant to explore similarity in xylem embolism resistance across plant organs.

Keywords Bordered pit · Electron microscopy · Pit membrane · Vessel · Wood anatomy

Martyna M. Kotowska and Rebecca Thom contributed equally to this manuscript.

✉ Martyna M. Kotowska
 martyna.kotowska@biologie.uni-goettingen.de

1 Institute of Systematic Botany and Ecology, Ulm University, Albert-Einstein-Allee 11, 89081 Ulm, Germany

2 Albrecht-von-Haller Institute for Plant Sciences, University of Goettingen, Untere Karspüle 2, 37073 Göttingen, Germany

3 Department of Biological Science, California State University Fullerton, 800 N. State College Blvd., Fullerton, CA 92831-3599, USA

Introduction

From the plant roots all the way to the minor veins in leaves, water follows the network of conduits through the xylem tissue typically under negative pressure. The passage from conduit to conduit happens through bordered pit membranes, which are responsible for most of the resistance along the hydraulic pathway (Sperry et al. 2006; Choat et al. 2008). It is poorly understood, however, whether these pit membranes of water-conducting cells in the xylem of particular organs differ in structural characteristics. Especially under conditions of drought, the xylem sap can be prone to bubble formation and the occurrence of embolism (Choat et al. 2012; Jansen and Schenk 2015). Since leaves are known to experience more negative water potentials than stems and roots, it has been suggested that xylem embolism develops more frequently in leaves than in other organs (Tyree and Ewers 1991). While available data provide strong evidence for embolism formation via air-seeding at bordered pits (Sperry and Tyree 1988; Brodribb et al. 2016; Schenk et al. 2017; Jansen et al. 2018), the ultrastructure of bordered pits

and their pit membranes has been studied at the whole plant level for only few woody angiosperm species (Klepsch et al. 2018; Pfautsch et al. 2018).

Given the finite length of water conducting cells in xylem, cell wall openings in conduits play a crucial role in hydraulic efficiency, enabling transport between adjacent conduits (Sperry and Tyree 1988; Choat et al. 2008). While perforation plates interconnect a series of vessel elements by complete openings in the secondary and primary wall, bordered pits between adjacent conduit walls represent an opening in the secondary wall only (Schacht 1859; Schmid and Machado 1968). The middle lamella and primary wall in bordered pits become modified during cell hydrolysis and develop into a porous pit membrane mainly composed of cellulose microfibrils (Bonner and Thomas 1972; Czaninski 1979; Herbette et al. 2014). Based on empirical and modelling work, intervessel pit membranes are suggested to account for more than 50% of the total xylem hydraulic resistance (Schulte and Gibson 1988; Sperry and Hacke 2004; Choat et al. 2006, 2008).

Within the water-conducting network, embolism resistance is a function of withstanding air entry and its propagation and was found to be associated with pit membrane thickness (Jansen et al. 2009; Lens et al. 2011). The pit membrane thickness can vary up to fivefold across angiosperms with species showing thin pit membranes typically having a higher vulnerability to embolism than species with thick pit membranes (Scholz et al. 2013; Li et al. 2016; Schuldt et al. 2016). Based on perfusion experiments with colloidal gold particles, pore sizes in pit membranes appear to be typically smaller than 20 nm (Choat et al. 2003, 2004; Zhang et al. 2017), but it is unknown if pit membrane thickness is related to pore size, which is one of the characteristics determining air-seeding pressure (Meyra et al. 2007; Jansen and Schenk 2015). Vulnerability to xylem embolism is reported to vary across organs and along a vertical or radial profile in various angiosperms (Alder et al. 1996; Domec and Gartner 2002; Choat et al. 2005; Burgess et al. 2006; Losso et al. 2019), with roots suggested to be more vulnerable to embolism than aboveground organs in various species (Sperry and Saliendra 1994; Alder et al. 1996; Kavanagh et al. 1999; McElrone et al. 2004). A negative relation between conduit size and embolism resistance has been suggested and is frequently assumed to explain temporal and spatial differences in intraspecific embolism resistance (Tyree and Sperry 1989; Hacke et al. 2000). However, no relationship between vessel diameter and embolism resistance was found for *Acer grandidentatum* (Alder et al. 1996), while similar vulnerability to embolism was also found between root, stem and leaf tissues of tomato (Skelton et al. 2017). Since mechanistic processes behind hydraulic resistance and vulnerability to embolism in plants are likely determined by variation in bordered pits and pit membrane structure (Domec et al. 2006; Scholz

et al. 2013), it seems reasonable to expect that pit membrane thickness, the size of pit membrane pores, or other bordered pit characteristics could explain potential variation in xylem embolism resistance within a tree.

Furthermore, pit membrane observations are complicated by potential preparation artefacts (e.g. Shane et al. 2000; Jansen et al. 2008; Tixier et al. 2014). Structural differences have been reported between dehydrated and wet, never-dried pit membranes (Pesacreta et al. 2005; Li et al. 2016; Zhang et al. 2017). In particular, shrinkage or even irreversible aspiration of the pit membranes to the roof of the pit chamber is a general concern, resulting in changes of pit membrane thickness and electron density under transmission electron microscopy (TEM), together with potential changes in pore size (Zhang et al. 2017). Wood samples that were air-dried, ethanol-stored, or frozen prior to TEM preparation showed intervessel pit membranes that were ca. 30% thinner and more electron dense than pit membranes in fresh samples (Li et al. 2016). Shrinkage of pit membranes also occurs under natural conditions in the field (Zhang et al. 2017).

Here, we explore the variation of intervessel pits and pit membranes at the intra-tree level for *Acer pseudoplatanus*, which has a moderate xylem embolism resistance (Lens et al. 2011). Although roots, stems, and leaves of this species are not known to differ in embolism resistance, a pronounced difference in pit membrane thickness between these organs could be indicative of the hydraulic vulnerability segmentation hypothesis (Zimmermann 1983; Tyree and Ewers 1991; Hochberg et al. 2016; Johnson et al. 2016). More specifically, we examined the pit structure and membrane thickness across various plant organs. While clear differences in vessel dimensions such as vessel surface area can be expected, we also expect quantitative differences in the morphology of bordered pits, with larger pits in wide conduits, and smaller ones in more narrow ones. Moreover, the effect of sample storage and dehydration on pit membrane shrinkage and aspiration was investigated for branch samples of *A. pseudoplatanus*. It is expected that dehydration increases the likelihood of pit membrane aspiration and pit membrane shrinkage.

Materials and methods

Plant material

Acer pseudoplatanus L. was selected as study species because it is a common species in the forest surrounding Ulm University. Its general wood anatomy, including vessel length distribution, bordered pit morphology, and chemical composition of pit membranes had been studied in earlier work (Lens et al. 2011; Nardini et al. 2012; Klepsch et al. 2016).

We based our intra-tree sampling on a single, mature and healthy tree of *A. pseudoplatanus* located at the Botanical Garden of Ulm (coordinates 48°25′17.37″N, 9°57′32.74″E) at an altitude of 594 m. The tree was approximately 15-m tall with a diameter of 13.5 cm at breast height, growing at the southern forest edge in a sun-exposed position, with a 3-m distance to surrounding trees. Samples were collected three times between May and July 2016 to include xylem from the vegetative organs.

Root segment samples were taken at a soil depth of 5–20 cm after tracing back the root to the main stem. We sampled both small-diameter roots (i.e. < 5 mm in diameter) and large-diameter roots (i.e. > 7 mm in diameter). An increment borer (Haglöf, Långsele, Sweden) was used for taking recent wood from the stem. Since the current grow ring was poorly developed, especially in May, we studied young stem xylem from the previous growth ring (i.e. developed in 2015). Older stem wood samples were collected at a depth of 5, 7 and 7.5 cm from the cambium. Since *A. pseudoplatanus* typically develops heartwood discolouration after trees reach a diameter at breast height of 45 cm (Kadunc 2007), the older samples collected do not represent true heartwood and are referred to as inner sapwood instead. All stem wood samples were collected at breast height, i.e. 60–100 cm above the ground. Sun-exposed branches (ca. 10 mm in diameter) were cut off at a height of 4.5–6 m using a pole pruner. The leaves investigated were taken from these branches, distinguishing xylem from the leaf petiole, leaf midrib, and secondary veins. All samples were placed into a bucket filled with water and brought back to the lab within ca. 30 min to prevent dehydration.

The potential preparation artefacts associated with pit membrane observations were studied on three branches taken from three individuals of *A. pseudoplatanus*, growing at the Botanical Garden of Ulm University. These branches were between 3 and 6 years old, with a diameter of 8–9 mm. From each branch, a straight internode was chosen, which was cut into three 2-cm-long stem segments.

The term "intervessel pit membrane" or "pit membrane" is used here in a broad sense to include vessel–tracheid and tracheid–tracheid pit membranes, which are structurally and functionally similar to vessel–vessel pit membranes (Schmid and Machado 1968).

Light microscopy

For light microscopy (LM), transverse sections of 20–30-µm thickness were made with a microtome (Schenkung Dapples MikroL) and stained with safranin and Astra Blue (Merck KGaA, Darmstadt, Germany). Sections were stained in safranin for 5 min, washed twice with distilled water for 30 s, and then immersed in Astra Blue for 45 min. After washing the sections once again in distilled water, they were dehydrated through an ethanol series, using 50%, 70% and 96% EtOH and Neo-Clear® (Merck Millipore) for 2 min each. The stained sections were then transferred to a microscope slide and embedded with Neo-Mount® (Merck Millipore). The slides were dried in an oven at 60 °C for 15 h. Photographs of transverse sections were taken with a microscope equipped with a digital camera (AXIOZoom V16, Carl Zeiss MicroImaging GmbH, Ulm, Germany) at 80× magnification. The images were processed using Adobe Photoshop CS2 (version 9.0. Adobe Systems Incorporated, USA) and analysed with ImageJ (version 1.50i) using the particle-analysis-function after applying a black-and-white threshold. ImageJ was also used to analyse SEM and TEM pictures. Single vessel diameters (D) were used to calculate the hydraulically weighted vessel diameter (D_H) according to Sperry et al. (1994) as $D_H = \Sigma D^5/\Sigma D^4$. A list of the parameters and abbreviations measured can be found in Table 1.

Scanning electron microscopy

For scanning electron microscopy (SEM), fresh samples were oven-dried at 60 °C for 15 h and split in a tangential plane. They were gold-coated with a Balzers Union sputtering device (Balzers Union, Balzers, Fürstentum Liechtenstein) for 2 min (Jansen et al. 2008). SEM studies were carried out with a Phenom XL microscope (Phenom-World, Eindhoven, The Netherlands) at an accelerating voltage of 5 kV. Special care was taken during SEM observations to distinguish intervessel pits from vessel–parenchyma pits.

Transmission electron microscopy

Longitudinal slivers of fresh xylem were cut into 1 mm × 1 mm × 2 mm segments, fixed in a glutaraldehyde solution (including 2.5% glutaraldehyde, 0.1 mol phosphate, 1% sucrose, pH 7.3). The samples were then washed three to four times in a phosphate buffer for 5–10 min each and post-fixed with a buffered 2% OsO_4 solution. Then, dehydration was performed with a propanol series (30, 50, 70, 90%) for 2–3 min each, and finally by three treatments with 100% propanol (30 min each). Samples were immersed in two solutions of 1.2-propylene oxide (CAS-Nr.75-56-9, Fontenay-sous-Bois Cedex) for 5–10 min each, and gradually embedded in epon resin (Sigma-Aldrich, Steinheim, Germany), which was polymerized at 60 °C for 48 h. Transverse, semi-thin sections of 500 nm thickness were cut with a Leica Ultracut UTC microtome (Leica Microsystems GmbH, Wetzlar, Germany). The sections were stained with 0.5% toluidine blue in 0.1-M phosphate buffer and mounted on microscope slides using Eukitt. For the TEM observations, ultra-thin sections of 60–80-nm thickness were prepared with the microtome and placed on copper grids (Grids 300 mesh,

Table 1 List of the xylem anatomical features measured, with reference to the microscope method and units

Acronym	Definition	Method	Units
A_{ap}	Pit aperture surface area	SEM	μm^2
AP_f	Aperture shape = longest pit aperture diameter (D_{long})/shortest pit aperture diameter (D_{short})	SEM	–
A_{pit}	Pit membrane surface area	SEM	μm^2
D	Conduit (vessel or tracheid) diameter	LM	μm
D_H	Hydraulically weighted conduit diameter	LM	μm
D_{long}	Longest diameter of the pit aperture	SEM	μm
D_{short}	Shortest diameter of the pit aperture	SEM	μm
F_{ap}	Aperture fraction = pit aperture surface area (A_{ap})/pit membrane surface area (A_{pit})	SEM	–
F_{Lumen}	Proportion of the conduit lumen area over the xylem area	LM	%
T_{PM}	Pit membrane thickness	TEM	μm
T_{VW}	Double conduit wall thickness between neighbouring conduits	LM and TEM	μm
u	Wood moisture	Water displacement method	%
VD	Conduit density, number of conduits per mm^2	LM	n/mm^2
VI	Vulnerability index = average conduit diameter/conduit density	LM	–

LM light microscope, *SEM* scanning electron microscopy, *TEM* transmission electron microscopy

Plano GmbH, Wetzlar, Germany). TEM work was done with a JEOL JEM-1400 TEM (Jeol Germany GmbH, Freising, Germany).

For each sample, 10–25 pits were imaged. Pit membranes and intervessel wall thickness were measured using ImageJ (version 1.50i, National Institutes of Health, Bethesda, MD, USA). Intervessel pit membrane thickness (T_{PM}, nm) was calculated as the mean value of three measurements at opposite sides near the pit membrane annulus and at the centre of the pit membrane. Measurements of the intervessel wall were based on semi-thin sections and excluded cell wall corners and bordered pits.

Effects of sample storage treatment

Samples for the treatment experiment were collected in May 2016 from three branches, which were between 3 and 6 years old, and 8 and 9 mm in diameter. Wood segments from the branch were split and the weight was measured using an analytical balance (Kern ABT 220-5DM, KERN and SOHN GmbH, Balingen, Germany). A total of 12 samples were treated given one of the drying or fixation treatments (Table 2). We applied the following five treatments: (1) no treatment (i.e. fresh, never-dried wood), (2) partial to complete dehydration, (3) short- to long-term ethanol storage, (4) immediate fixation in glutaraldehyde fixative, and (5) formaldehyde storage. After one of these pre-treatments, samples were prepared for TEM following the same approach as described above. Wood moisture content and tissue density were calculated as proportion of initial weight and volume to oven-dry weight after drying at 103 °C.

Table 2 List of the various storage and preparation treatments applied to branch xylem samples of *Acer pseudoplanatus* before samples were fixed and embedded for transmission electron microscopy

Abbreviation	Treatment	Duration
C	Fresh	–
D1	Air-drying on lab bench	1 h, 15 min
D3	Air-drying on lab bench	3 h
D4	Air-drying on lab bench	4 h, 30 min
Da	Air-drying on lab	3 days
Do	Oven-drying (100 °C)	3 days
E1	Ethanol (70%)	5 h
E24	Ethanol (70%)	24 days
FA	Formaldehyde	24 days

Statistical analyses

Correlations between morphological bordered pit characteristics were calculated by determining Pearson's correlation coefficient using the '*ltm*' package in R version 3.3.2 (R Development Core Team, 2016). When linear relationships between characters were assumed, a Q–Q plot was used to test the residuals for normal distribution and homoscedasticity. Mixed effect models were used in case repeated measures were taken from the same sample or section from TEM measurements. Here, the *lme* function from the package '*nlme*' was used, with sample or section as random factor. To calculate differences between organs, either the Kruskal–Wallis test (package: '*pgirmess*' Giraudoux 2017), or the Tukey HSD test (*glht* package: '*multcomp*') were used, depending on whether the residuals were normally

distributed. We tested the effects of organ, sample as well as microscopic picture section or membrane location on the measured morphological pit variables with an analysis of variance (ANOVA). We calculated the proportion of the variance explained by organ, sample, section or location and residual effect as $\sigma^2_{\text{effect}}/\sigma^2_{\text{total}}$.

Results

Variation in vessel characteristics

Vessel dimensions varied distinctly across the plant organs studied, especially with respect to vessel diameter (Table A1; Fig. A1). The widest vessels were observed in large root samples (vessel diameter $D = 53.2 \pm 13.7$ μm; hydraulically weighted vessel diameter $D_H = 98.0 \pm 19.5$ μm), while much narrower vessels occurred in the xylem of the leaf midrib ($D = 16.3 \pm 1.6$ μm and $D_H = 18.9 \pm 2.4$ μm). Narrow vessels were densely packed with vessel density values up to 1144.91 ± 22.88 n/mm^2 in the leaf midrib. The vessel density was also remarkably high in small-diameter roots compared to other plant organs (197.62 ± 110.48 n/mm^2). In the stem and branch samples, where vessels were neither densely arranged nor extremely wide, the xylem area occupied by vessels was rather small compared to root and leaf samples. The conduit lumen fraction per total xylem area (F_{Lumen}) was highest in the leaves, with 21.85 ± 5.41 in the leaf petiole and 25.61 ± 4.66 in the midrib, respectively. Also, the vulnerability index (average vessel diameter/vessel density; VI) was highest in outer sapwood and large root samples (1.26 ± 0.23 and 1.26 ± 0.23, respectively).

Intratree variation in bordered pit morphology

Scanning electron microscopy observations showed considerable differences in the size and shape of bordered pits between the plant organs observed (Fig. A2). The size of the pit area (A_{pit}, μm^2) was distinctly different between all organs (Table A1; Fig. 2b). In young roots, the pits had a relatively small area with an average of 28.47 μm^2. A_{pit} values increased for large roots, and the largest pits were found in the outer sapwood (50.16 ± 14.11 μm^2). Bordered pits were smallest for the leaf midrib, with an average value of 11.97 ± 6.38 μm^2 (Table A2).

Pit aperture areas (A_{ap}, μm^2) were relatively small in the young roots as well as in leaf samples, with a mean value of 1.73 ± 0.98 μm^2 for the leaf midrib (Fig. 2c). Highest A_{ap} values were measured in the large roots (4.11 ± 1.10 μm^2), despite the fact that their pit membrane areas were only intermediate in size. Pit apertures in xylem of the trunk and branches had roughly the same size of ca. 3.5 μm^2.

Pit apertures showed different shapes, ranging from slit-like long openings to almost circular apertures covering only a small area of the pit. In the roots, the longest pit aperture diameters were about threefold longer than the shortest diameters, while this ratio (AP$_f$, defined as the longest pit aperture diameter divided by the shortest pit aperture diameter) was about 2 for pit apertures in the branches. In the leaves, however, pit apertures became more elongated again. High AP$_f$ values of 3.36 ± 0.11 were measured for the leaf midrib. However, there was considerable variation in pit aperture shape within a leaf, with oval to nearly circular apertures in the leaf petiole (Fig. A2). AP$_f$ values of the outer sapwood differed significantly between the root samples and the leaf midrib.

The pit area (A_{pit}) and pit aperture area (A_{ap}) varied independent of each other among plant organs, which was shown by the pit aperture fraction (F_{ap}, defined as $A_{\text{pit}}/A_{\text{ap}}$). The lowest F_{ap} values were found in the outer sapwood (0.08 ± 0.04), followed by branches and small root samples ($F_{\text{ap}} = 0.10 \pm 0.03$ and 0.11 ± 0.08, respectively). The highest F_{ap} values were found in the leaves, with a mean value of 0.43 ± 0.45 for leaf petioles, which was 5 times as high as the F_{ap} measured for the outer wood (Table A1; Fig. A2).

Intratree variation in pit membrane structure

Pit membranes in intervessel pits could be clearly observed under TEM after post-fixation with OsO$_4$, which resulted in a granular, electron dense appearance of the pit membrane (Fig. 1). In most cases, the largest electron dense particles occurred on the outermost sides of the pit membrane. A clearly different OsO$_4$ staining was observed in a few developing vessels before cell hydrolysis. These pit membranes showed a fairly homogeneous structure without dark particles. Moreover, there was considerable variation in the electron density of the pit membranes in fully developed vessels. In some cases, the electron dense particles showed an irregular, non-homogeneous distribution, while a lamellar, grey appearance was observed for the middle lamella.

Pit membrane thickness (T_{PM}, nm) as observed by TEM varied by 46% between leaf veins and outer sapwood (214 ± 19 nm and 384 ± 51 nm, respectively; Table A1). The thickness of membranes generally increased from the roots towards the sapwood and decreased towards the secondary veins in the leaves (Fig. 2). The highest values were found in the outer sapwood, while the thickest pit membranes in the leaf were located in the midrib (Table A1). T_{PM} in the sapwood samples differed significantly from all other organs, with both the outer and inner sapwood being different from petioles and secondary veins as well as young roots (Fig. 2a).

Intervessel wall thickness (T_{VW}, μm) followed a similar trend across the tree as pit membrane thickness values. T_{VW} was on average 4.61 ± 1.02 μm in the young roots, and up to
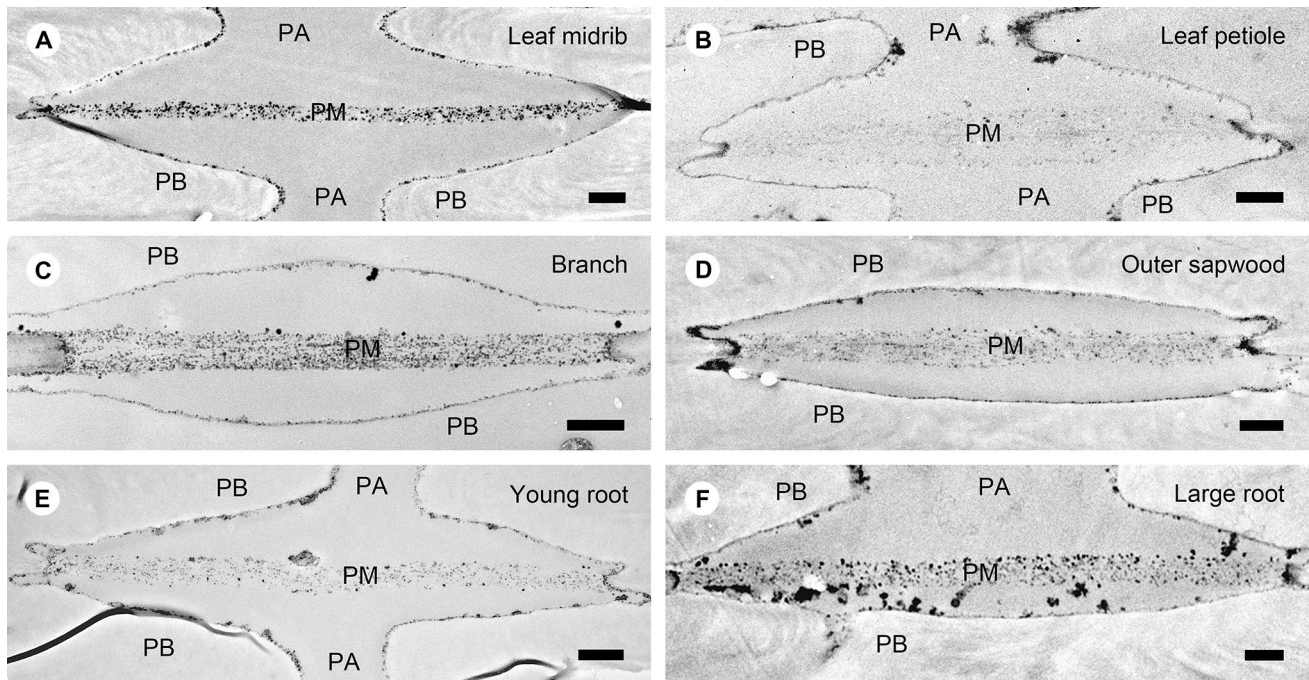
Fig. 1 Transmission electron microscopy (TEM) images showing intra-tree variation of intervessel pit membranes in xylem tissue of *A. pseudoplatanus*: **a** leaf midrib; **b** leaf petiole; **c** branch; **d** outer sap-

wood; **e** young root; **f** large root. *PA* pit aperture, *PM* pit membrane, *PB* pit border. Scale bar = 500 nm

6.85 ± 1.06 µm in the large root. The smallest T_{VW} values were found in the leaves with a minimum of 3.08 ± 0.31 µm in the secondary leaf vein (Table A1). Considering the effect of sample identify as a random factor, there was no significant correlation between T_{VW} and T_{PM}, although pits in vessels with thin walls (e.g. in the leaves) generally had thinner membranes than those of vessels with thick walls, as could be found in the large root and the outer wood (Fig. 3a, b). Also, vessel surface area was not significantly related to T_{PM} (lme; sample as random factor, $p = 0.3$), indicating that pit membranes were not thicker when the vessel size increases. However, a hump-shaped distribution between vessel surface area and T_{PM} was found (Fig. 3).

The variance in the measured pit morphological and functional characteristics differed markedly between the parameters (Fig. A3). Organ identity explained between 20% and >90% of the variance in the dataset. While tissue density and T_{VW} appeared to be determined mainly by the organ, residual variance in T_{PM} and pit morphology (A_{pit} and A_{ap}) was dominating. Sample identity and location of membrane measurements explained jointly not more than 8% of the variance.

Influence of sample treatment on pit membrane thickness

We found a strong impact of wood moisture and sample storage treatment on pit membrane thickness, an effect

that was observed to be irreversible. T_{PM} was linearly decreasing with wood moisture (Fig. 4a). The average thickness of membranes in dehydrated samples was reduced by 73% in oven-dried, 27% in air-dried, and 23% in ethanol treated samples as compared to pit membranes in fully hydrated, fresh wood (Fig. 4b).

In fresh branch samples, pit membranes were usually straight with only some exceptions being slightly strained, indicating that they were well hydrated (Fig. 5). Average T_{PM} in dried samples was reduced, while the number of strained and aspirated membranes increased (Fig. 4b). All dried samples differed significantly in their aspiration amount from the fresh ones ($p < 0.05$; Kruskal–Wallis test). In the oven-dried sample, nearly all pit membranes were aspirated (Figs. 4b, 5d), and their T_{PM} values were significantly different from all other samples.

The results for the samples stored in ethanol for 1 day were similar to those of the fresh samples, whereas samples kept in ethanol for 3 weeks showed significantly thinner pit membranes. The samples stored in formaldehyde for 3 weeks showed no significant difference to the fresh ones. However, pit membranes treated with formaldehyde appeared to be more electron dense in TEM than fresh ones (Fig. 5f).
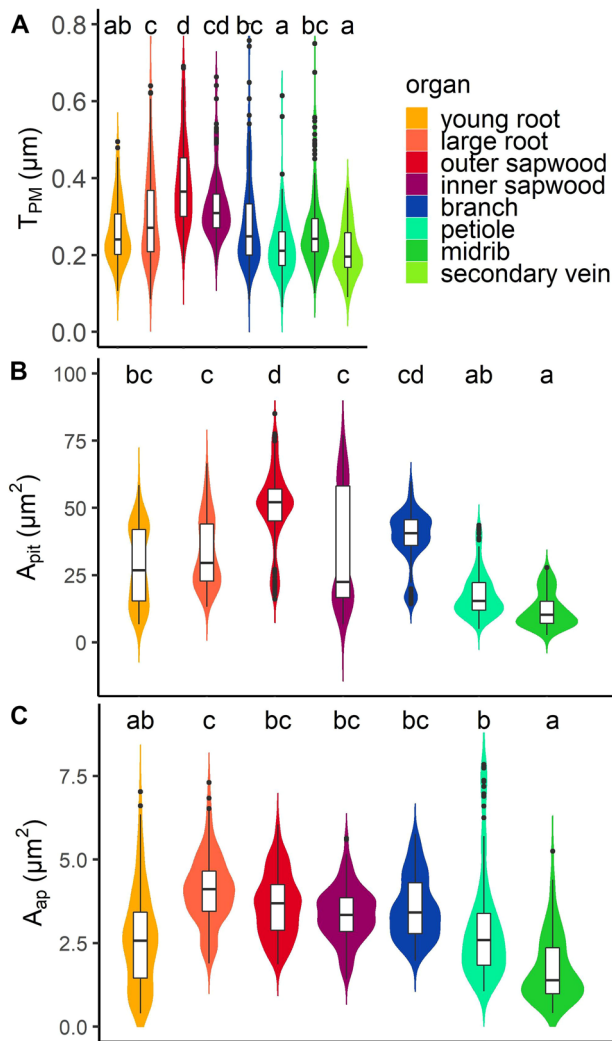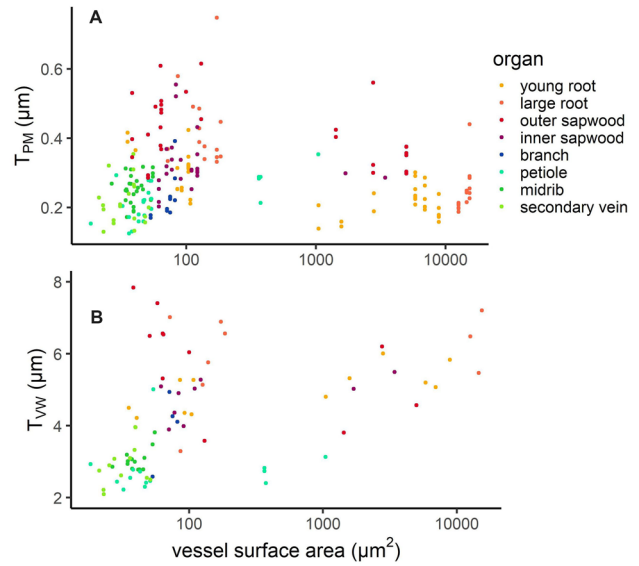
Fig. 2 Comparison of intervessel pit membrane characteristics in xylem tissue from various organs of *A. pseudoplatanus*: **a** pit membrane thickness (T_{PM}), **b** pit membrane surface area (A_{pit}), **c** pit aperture surface area (A_{ap}). Violin plot showing median and the interquartile range with probability density of the data. Letters indicate significant differences across organs (HSD-Tukey test)

Fig. 3 The relationship between **a** pit membrane thickness (T_{PM}) and vessel surface area; **b** vessel wall thickness (T_{VW}) and vessel surface area for xylem tissue from various organs of *A. pseudoplatanus*
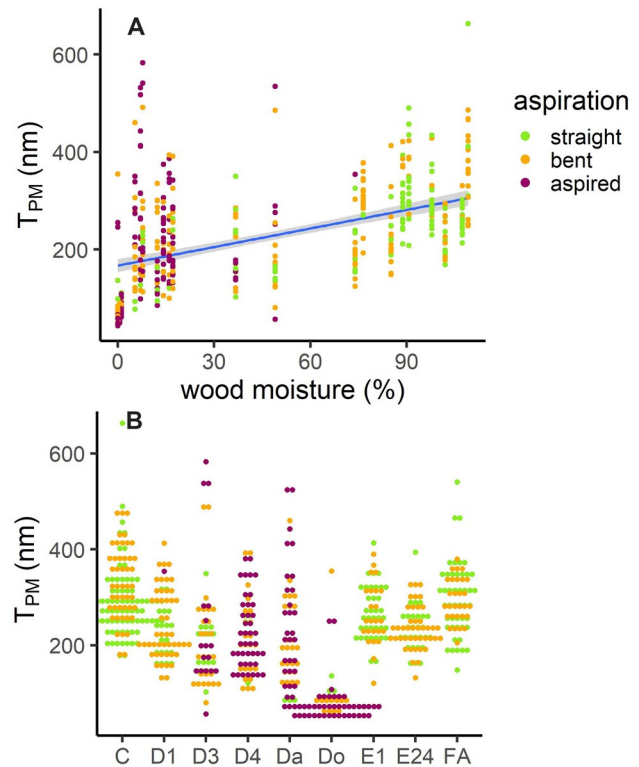
Fig. 4 The influence of **a** wood moisture content (%) in relation to pit membrane thickness (T_{PM}) in successively dried wood samples of *A. pseudoplatanus* ($p < 0.001$, $r^2 = 0.188$). Three conditions of pit membrane aspiration were distinguished; and **b** treatment prior to standard TEM preparation (see Table 2 for abbreviations) on pit membrane thickness (T_{PM}), and the degree of pit membrane aspiration in sapwood samples of *A. pseudoplatanus*

Discussion

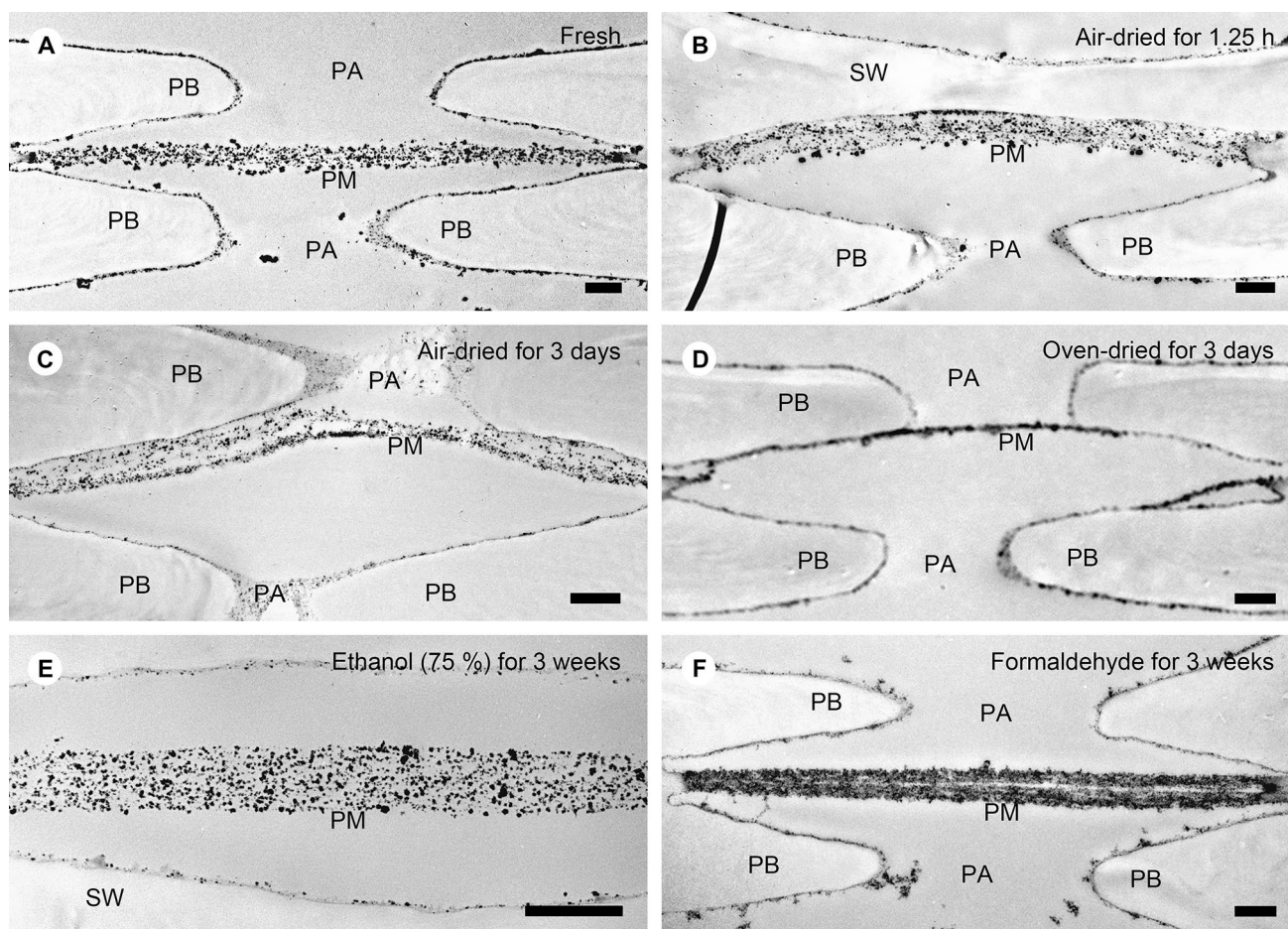### Intratree variation in pit morphology

The findings for *A. pseudoplatanus* show that pit membranes of different organs within a tree display considerable similarities in their general structure, although quantitative differences in pit membrane thickness and morphology occur both within and across organs. The most pronounced difference between organs was present in hydraulically relevant characteristics. Conduit diameters as well as densities show the highest variability along the hydraulic pathway with differences of more than tenfold in density and around fivefold for diameter. While small and narrow vessels are usually found

Fig. 5 Transmission electron microscopy (TEM) images of intervessel pit membranes in sapwood of *A. pseudoplatanus* showing interconduit pit membranes with different treatments: **a** pit membrane in non-dried, freshly embedded sample; **b** air-dried for 1.25 h; **c** air-dried for 3 days; **d** oven-dried for 3 days; **e** stored in 70% ethanol over 3 weeks; **f** stored in formaldehyde for 3 weeks. *PB* pit bordered, *PA* pit aperture, *PM* pit membrane. Scale bar = 500 nm

in the leaf xylem, the conduit diameter increases towards the stem and the largest vessels are found in roots (Anfodillo et al. 2013). Vessel tapering is a well-known phenomenon and has been shown for numerous temperate as well as tropical tree species (Martinez-Vilalta et al. 2002; Olson et al. 2014; Kotowska et al. 2015). Since vessel diameter is associated with vessel length (Hacke et al. 2006; Liu et al. 2018), it is likely that wide vessels in the roots and stems of *A. pseudoplatanus* are longer than those in the xylem tissue of branches and leaves.

Unlike conduit dimensions, pit membrane area shows a less pronounced variation among the organs. Here, we observed the highest values in outer sapwood, while smaller pit and aperture sizes were found at the distal sides of the flow path, namely towards leaves and small-diameter roots. A similar pattern was observed for pit aperture area, but with A_{ap} values highest in large root samples. It is possible that dimensions of pit membrane area and pit aperture area are at least partly affected by conduit dimensions, which may also

indicate that the bordered pit hydraulic resistance shows a more or less constant proportion to the vessel lumen resistance (Choat et al. 2008). However, the variability within each organ was very high and significant differences were found only between the extreme ends of the spectrum, i.e. between leaf midribs and sapwood or large roots.

A hump-shaped distribution was also mirrored in the pit membrane thickness, which was highest in outer sapwood. Slightly thinner pit membranes were found in inner wood, and about 40% thinner pit membranes occurred in leaves. Differences between inner and outer sapwood could be caused by natural shrinkage when vessels embolise, are no longer functional, and pit membranes becomes dry up. Pit membrane shrinkage might be caused by alteration of hydrogen bonds between glucose chains of cellulose molecules after removal of water molecules (Fang and Catchmark 2014; Martinez-Sanz et al. 2017).

It is largely unknown how long it takes for pit membranes to undergo shrinkage. Our observations of bench dehydrated

samples show that 1–4 h has considerable consequences for pit membrane shrinkage, although there is a very large variation in pit membrane thickness, with some pit membranes seriously shrunken, and others only partly or weakly affected (Figs. 4b, 5c). Whether or not this variation can be explained by simultaneous embolism occurrence and/or mechanical stretching of the pit membrane against the pit border remains to be tested.

We tested the hypothesis that pit membrane thickness is linked to vessel size. However, we found that vessel size was not significantly related to T_{PM} across plant organs (Fig. 3a). Although T_{PM} increases with conduit size for very narrow conduits, the thickness decreases slightly for larger conduits in root and sapwood samples with a lumen surface area above 1000 μm^2. The observation that narrow and wide conduits are largely similar in their pit membrane thickness may indicate that a potential difference in drought-induced embolism between wide and narrow conduits is not driven by pit membrane quality but by quantity, as postulated by the rare pit hypothesis (Wheeler et al. 2005; Hacke et al. 2006). Yet, even pit membrane quantity as pit area per vessel was not found to correlate with embolism resistance across seven *Acer* species (Lens et al. 2011). Interestingly, we found a stronger link between intervessel wall thickness and vessel surface area than with T_{PM} (Fig. 3b), but also here the relationship was not significant. While larger conduits would need stronger walls to avoid wall implosion (Hacke et al. 2001), other cell wall characteristics such as chemical composition and cellulose fibril arrangement are likely to determine the mechanical properties of conduit walls (Butterfield 1998; Pereira et al. 2018).

Preparation artefacts related to pit membrane thickness

As most scientific measurements cannot be conducted in the field, it is important to consider how samples can be stored and transported in an efficient and uncomplicated way. Traditionally, wood samples collected in the field are either dried or stored in ethanol for long-term conservation. Here, we have investigated how different sample storage treatments influence the pit membrane thickness of intervessel pits. We found strong influence of the type of treatment and the storage duration, with pit membrane thickness considerably decreasing by dehydration of the sample. This dehydration process was found to be largely irreversible, because rehydration for TEM preparation did not seem to restore the pit membrane in its original thickness. This finding is in agreement with earlier research, suggesting that dried-rehydrated pit membranes were about 40–60% thinner than fresh (non-dried) pit membranes (Pesacreta et al. 2005; Scholz et al. 2013; Li et al. 2016; Zhang et al. 2017).

Furthermore, gradual dehydration of wood samples was found to be associated with an increasing frequency of aspirated and shrunken pit membranes. Pit membranes in completely air-dried and oven-dried samples were found to show the highest amount of aspirated and the thinnest pit membranes. Likewise, long-term ethanol storage decreased T_{PM} by more than 20%, which is similar to the effect of air-drying. Only formaldehyde treatment did not have a significant influence on pit membrane thickness, and thus seems an alternative option. However, formaldehyde reacts primarily with proteins by reaction with nitrogen or other atoms of proteins, while other molecules such as lipids can be trapped in a matrix of cross-linked proteins. It is likely that the protein fixation by formaldehyde also leads to artificial penetration of various substances into the pit membrane. Therefore, formaldehyde strongly affects the electron density of the pit membranes in TEM, which results in darker pit membranes under TEM.

These findings underline the necessity to observe similarly treated samples for TEM to ensure comparable results. Ideally, completely fresh and hydrated samples should be given priority over stored samples. Nonetheless, even freshly embedded samples are dehydrated by any standard preparation method for TEM, because resin embedding cannot be avoided without alcohol treatment. Interestingly, comparisons of pit membrane thickness measured under TEM and fully hydrated pit membranes under confocal laser scanning microscopy suggest that fully hydrated pit membranes may be much thicker than pit membranes in TEM samples (Schenk et al. 2018). Besides a broader sampling both at the intraspecific and interspecific level, more research is needed to investigate the degree to which pit membranes effectively dehydrate in the field by desiccation, and to examine the spatial distribution of pit membrane shrinkage in living plants. The finding that shrinkage of pit membranes is largely irreversible and possibly associated with changes in pore volume fraction (Zhang et al. unpublished data) raises also questions about embolism refilling and potential consequences for water transport.

References

Alder NN, Sperry JS, Pockman WT (1996) Root and stem xylem embolism, stomatal conductance, and leaf turgor in *Acer grandidentatum* populations along a soil moisture gradient. Oecologia 105:293–301

Anfodillo T, Petit G, Crivellaro A (2013) Axial conduit widening in woody species: a still neglected anatomical pattern. IAWA J 34:352–364. https://doi.org/10.1163/22941932-00000030

Bonner LD, Thomas RJ (1972) The ultrastructure of intercellular passageways in vessels of yellow poplar (*Liriodendron tulipifera*, L.) part I: vessel pitting. Wood Sci Technol 6:196–203

Brodribb TJ, Skelton RP, McAdam SAM et al (2016) Visual quantification of embolism reveals leaf vulnerability to hydraulic failure. New Phytol 209:1403–1409

Burgess SSO, Pittermann J, Dawson TE (2006) Hydraulic efficiency and safety of branch xylem increases with height in *Sequoia sempervirens* (D. Don) crowns. Plant Cell Environ 29:229–239

Butterfield BG (1998) Microfibril angle in wood. In: The Proceedings of the IAWA/IUFRO international workshop on the significance of microfibril angle to wood quality. International Association of Wood Anatomists, Westport

Choat B, Ball M, Luly J, Holtum J (2003) Pit membrane porosity and water stress-induced cavitation in four co-existing dry rainforest tree species. Plant Physiol 131:41–48

Choat B, Jansen S, Zwieniecki MA et al (2004) Changes in pit membrane porosity due to deflection and stretching: the role of vestured pits. J Exp Bot 55:1569–1575

Choat B, Lahr EC, Melcher PJ et al (2005) The spatial pattern of air seeding thresholds in mature sugar maple trees. Plant Cell Environ 28:1082–1089

Choat B, Brodie TW, Cobb AR et al (2006) Direct measurements of intervessel pit membrane hydraulic resistance in two angiosperm tree species. Am J Bot 93:993–1000

Choat B, Cobb AR, Jansen S (2008) Structure and function of bordered pits: new discoveries and impacts on whole-plant hydraulic function. New Phytol 177:608–626

Choat B, Jansen S, Brodribb TJ et al (2012) Global convergence in the vulnerability of forests to drought. Nature 491:752

Czaninski Y (1979) Cytochimie ultrastructurale des parois du xyleme secondaire. Biol Cell 35:97–102

Domec JC, Gartner BL (2002) Age-and position-related changes in hydraulic versus mechanical dysfunction of xylem: inferring the design criteria for Douglas-fir wood structure. Tree Physiol 22:91–104

Domec J-C, Lachenbruch B, Meinzer FC (2006) Bordered pit structure and function determine spatial patterns of air-seeding thresholds in xylem of Douglas-fir (*Pseudotsuga menziesii*; Pinaceae) trees. Am J Bot 93:1588–1600

Fang L, Catchmark JM (2014) Characterization of water-soluble exopolysaccharides from *Gluconacetobacter xylinus* and their impacts on bacterial cellulose crystallization and ribbon assembly. Cellulose 21:3965–3978

Giraudoux P (2017) "pgirmess": data analysis in ecology. R package version 1.6.7. https://CRAN.R-project.org/package=pgirmess

Hacke UG, Sperry JS, Pittermann J (2000) Drought experience and cavitation resistance in six shrubs from the Great Basin, Utah. Basic Appl Ecol 1:31–41

Hacke UG, Sperry JS, Pockman WT et al (2001) Trends in wood density and structure are linked to prevention of xylem implosion by negative pressure. Oecologia 126:457–461. https://doi.org/10.1007/s004420100628

Hacke UG, Sperry JS, Wheeler JK, Castro L (2006) Scaling of angiosperm xylem structure with safety and efficiency. Tree Physiol 26:689–701

Herbette S, Bouchet B, Brunel N et al (2014) Immunolabelling of intervessel pits for polysaccharides and lignin helps in understanding their hydraulic properties in *Populus tremula × alba*. Ann Bot 115:187–199

Hochberg U, Albuquerque C, Rachmilevitch S et al (2016) Grapevine petioles are more sensitive to drought induced embolism than stems: evidence from in vivo MRI and microcomputed tomography observations of hydraulic vulnerability segmentation. Plant Cell Environ 39:1886–1894

Jansen S, Schenk HJ (2015) On the ascent of sap in the presence of bubbles. Am J Bot 102:1561–1563

Jansen S, Pletsers A, Sano Y (2008) The effect of preparation techniques on SEM-imaging of pit membranes. IAWA J 29:161–178

Jansen S, Choat B, Pletsers A (2009) Morphological variation of intervessel pit membranes and implications to xylem function in angiosperms. Am J Bot 96:409–419

Jansen S, Klepsch M, Li S et al (2018) Challenges in understanding air-seeding in angiosperm xylem. Acta Hortic 1222:13–20

Johnson DM, Wortemann R, McCulloh KA et al (2016) A test of the hydraulic vulnerability segmentation hypothesis in angiosperm and conifer tree species. Tree Physiol 36:983–993

Kadunc A (2007) Factors influencing the formation of heartwood discolouration in sycamore (*Acer pseudoplatanus* L.). Eur J For Res 126:349–358

Kavanagh KL, Bond BJ, Aitken SN et al (1999) Shoot and root vulnerability to xylem cavitation in four populations of Douglas-fir seedlings. Tree Physiol 19:31–37

Klepsch MM, Schmitt M, Paul Knox J, Jansen S (2016) The chemical identity of intervessel pit membranes in Acer challenges hydrogel control of xylem hydraulic conductivity. AoB Plants. https://doi.org/10.1093/aobpla/plw052

Klepsch M, Zhang Y, Kotowska MM et al (2018) Is xylem of angiosperm leaves less resistant to embolism than branches? Insights from microCT, hydraulics, and anatomy. J Exp Bot 69:5611–5623

Kotowska MM, Hertel D, Abou Rajab Y et al (2015) Patterns in hydraulic architecture from roots to branches in six tropical tree species from cacao agroforestry and their relation to wood density and stem growth. Front Plant Sci 6:191

Lens F, Sperry JS, Christman MA et al (2011) Testing hypotheses that link wood anatomy to cavitation resistance and hydraulic conductivity in the genus *Acer*. New Phytol 190:709–723. https://doi.org/10.1111/j.1469-8137.2010.03518.x

Li S, Lens F, Espino S et al (2016) Intervessel pit membrane thickness as a key determinant of embolism resistance in angiosperm xylem. IAWA J 37:152–171

Liu M, Pan R, Tyree MT (2018) Intra-specific relationship between vessel length and vessel diameter of four species with long-to-short species-average vessel lengths: further validation of the computation algorithm. Trees 32:51–60

Losso A, Bär A, Dämon B et al (2019) Insights from in vivo micro-CT analysis: testing the hydraulic vulnerability segmentation in *Acer pseudoplatanus* and *Fagus sylvatica* seedlings. New Phytol 221:1831–1842

Martinez-Sanz M, Pettolino F, Flanagan B et al (2017) Structure of cellulose microfibrils in mature cotton fibres. Carbohydr Polym 175:450–463

Martinez-Vilalta J, Prat E, Oliveras I, Pinol J (2002) Xylem hydraulic properties of roots and stems of nine Mediterranean woody species. Oecologia 133:19–29. https://doi.org/10.1007/s00442-002-1009-2

McElrone AJ, Pockman WT, Martinez-Vilalta J, Jackson RB (2004) Variation in xylem structure and function in stems and roots of trees to 20 m depth. New Phytol 163:507–517. https://doi.org/10.1111/j.1469-8137.2004.01127.x

Meyra AG, Kuz VA, Zarragoicoechea GJ (2007) Geometrical and physicochemical considerations of the pit membrane in relation to air seeding: the pit membrane as a capillary valve. Tree Physiol 27:1401–1405

Nardini A, Dimasi F, Klepsch M, Jansen S (2012) Ion-mediated enhancement of xylem hydraulic conductivity in four *Acer* species: relationships with ecological and anatomical features. Tree Physiol 32:1434–1441

Olson ME, Anfodillo T, Rosell JA et al (2014) Universal hydraulics of the flowering plants: vessel diameter scales with stem length across angiosperm lineages, habits and climates. Ecol Lett 17:988–997

Pereira L, Domingues-Junior AP, Jansen S et al (2018) Is embolism resistance in plant xylem associated with quantity and characteristics of lignin? Trees 32:349–358

Pesacreta TC, Groom LH, Rials TG (2005) Atomic force microscopy of the intervessel pit membrane in the stem of *Sapium sebiferum* (Euphorbiaceae). IAWA J 26:397–426

Pfautsch S, Aspinwall MJ, Drake JE et al (2018) Traits and trade-offs in whole-tree hydraulic architecture along the vertical axis of *Eucalyptus grandis*. Ann Bot 121:129–141

Schacht H (1859) Über die Tüpfel der Gefäss-und Holzzellen. Bot Zeitung 17:238–239

Schenk HJ, Espino S, Romo DM et al (2017) Xylem surfactants introduce a new element to the cohesion-tension theory. Plant Physiol 173:1177–1196

Schenk HJ, Espino S, Rich-Cavazos SM, Jansen S (2018) From the sap's perspective: the nature of vessel surfaces in angiosperm xylem. Am J Bot 105:172–185

Schmid R, Machado RD (1968) Pit membranes in hardwoods—fine structure and development. Protoplasma 66:185–204

Scholz A, Rabaey D, Stein A et al (2013) The evolution and function of vessel and pit characters with respect to cavitation resistance across 10 *Prunus* species. Tree Physiol 33:684–694. https://doi.org/10.1093/treephys/tpt050

Schuldt B, Knutzen F, Delzon S et al (2016) How adaptable is the hydraulic system of European beech in the face of climate change-related precipitation reduction? New Phytol 210:443–458

Schulte PJ, Gibson AC (1988) Hydraulic conductance and tracheid anatomy in six species of extant seed plants. Can J Bot 66:1073–1079

Shane MW, McCully ME, Canny MJ (2000) Architecture of branch–root junctions in maize: structure of the connecting xylem and the porosity of pit membranes. Ann Bot 85:613–624

Skelton RP, Brodribb TJ, Choat B (2017) Casting light on xylem vulnerability in an herbaceous species reveals a lack of segmentation. New Phytol 214:561–569

Sperry JS, Hacke UG (2004) Analysis of circular bordered pit function I. Angiosperm vessels with homogenous pit membranes. Am J Bot 91:369–385

Sperry JS, Saliendra NZ (1994) Intra-plant and inter-plant variation in xylem cavitation in *Betula occidentalis*. Plant Cell Environ 17:1233–1241. https://doi.org/10.1111/j.1365-3040.1994.tb02021.x

Sperry JS, Tyree MT (1988) Mechanism of water stress-induced xylem embolism. Plant Physiol 88:581–587

Sperry JS, Hacke UG, Pittermann J (2006) Size and function in conifer tracheids and angiosperm vessels. Am J Bot 93:1490–1500

Sperry JS, Nichols KL, Sullivan JE, Eastlack SE (1994) Xylem embolism in ring-porous, diffuse-porous, and coniferous trees of northern Utah and interior Alaska. Ecology 75(6):1736–1752

Tixier A, Herbette S, Jansen S et al (2014) Modelling the mechanical behaviour of pit membranes in bordered pits with respect to cavitation resistance in angiosperms. Ann Bot 114:325–334

Tyree MT, Ewers FW (1991) The hydraulic architecture of trees and other woody plants. New Phytol 119:345–360. https://doi.org/10.1111/j.1469-8137.1991.tb00035.x

Tyree MT, Sperry JS (1989) Vulnerability of xylem to cavitation and embolism. Annu Rev Plant Biol 40:19–36

Wheeler JK, Sperry JS, Hacke UG, Hoang N (2005) Inter-vessel pitting and cavitation in woody Rosaceae and other vesselled plants: a basis for a safety versus efficiency trade-off in xylem transport. Plant Cell Environ 28:800–812. https://doi.org/10.1111/j.1365-3040.2005.01330.x

Zhang Y, Klepsch M, Jansen S (2017) Bordered pits in xylem of vesselless angiosperms and their possible misinterpretation as perforation plates. Plant Cell Environ 40:2133–2146

Zimmermann MH (1983) Xylem structure and the ascent of sap. Springer, New York